HYPERRIDE
THE FUTURE OF POWER DISTRIBUTION

Hybrid Provision of Energy based on Reliability and Resiliency by Integration of Dc Equipment

Work Package WP3

Hybrid Grid Enabling Solutions

Deliverable D3.12

Control Algorithms Implementation for LVACDC Active Frontend

Funding Instrument:	Innovation Action
Call:	H2020-LC-SC3-2020-EC-ES-SCC
Call Topic:	LC-SC3-ES-10-2020 - DC – AC/DC hybrid grid for a modular, resilient and high RES share grid development
Project Start:	1 October 2020
Project Duration:	48 months
Beneficiary in Charge:	AIT Austrian Institute of Technology GmbH (AIT)
Document Identifier:	doi:10.5281/zenodo.5115844

Dissemination Level		
PU	Public	✓
PP	Restricted to other programme participants (including the Commission Services)	
RE	Restricted to a group specified by the Consortium (including the Commission Services)	
CO	Confidential, only for members of the Consortium (including the Commission Services)	

This project has received funding from the European Union's Horizon 2020 research and innovation programme under Grant Agreement No. 957788.

Deliverable Information

Document Administrative Information	
Project Acronym:	HYPERRIDE
Project Number:	957788
Deliverable Number:	D3.12
Deliverable Full Title:	Control Algorithms Implementation for LVACDC Active Frontend
Deliverable Short Title:	Frontend Control Algorithms Implementation
Document Identifier:	HYPERRIDE-D312-FrontendControlAlgorithmsImplementation-submitted
Beneficiary in Charge:	AIT Austrian Institute of Technology GmbH (AIT)
Report Version:	v1.6
Contractual Date:	30/05/2021
Report Submission Date:	27/07/2021
Dissemination Level:	PU
Nature:	Demonstrator
Lead Author(s):	Anja Banjac (AIT), Philipp Svec (AIT)
Co-author(s):	Zoran Miletic (AIT), Johannes Stöckl (AIT)
Keywords:	ACDC hybrid grid, active frontend, DC droop control, AIT Smart Grid Converter, controller hardware-in-the-loop, European Union (EU), H2020, Project, HYPERRIDE, GA 957788
Status:	__ draft, __ final, _x_ submitted

Change Log

Date	Version	Author/Editor	Summary of Changes Made
25/11/2020	v1.0	T. Strasser (AIT)	Initial document
18/05/2021	v1.1	J. Stöckl (AIT)	Initial document structure, first inputs
09/06/2021	v1.2	A. Banjac, G. Jambrich, Z. Miletic, J. Stöckl, P. Svec (AIT)	Further inputs and refinements, final draft for review
17/06/2021	v1.3	T. Bragatto (ASM Terni Spa)	Review and improvements
18/06/2021	v1.4	P. Kopejtko (Eaton)	Review and improvements
15/07/2021	v1.5	A. Banjac, J. Stöckl, P. Svec (AIT)	Update and improvements
27/07/2021	v1.6	G. Jambrich, T. Strasser (AIT)	Final version

Table of Contents

List of Figures

List of Tables

List of Abbreviations

AC	Alternating Current
ACDC	Alternating Current and Direct Current
AFE	Active Front End
ASGC	AIT Smart Grid Converter
BES	Battery Energy Storage
C-HIL	Controller Hardware-in-the-loop
CLI	Command Line Interface
DC	Direct Current
DoA	Description of Action
EV	Electric Vehicle
HIL	Hardware-in-the-loop
LVAC	Low Voltage Alternating Current
LVACDC	Low Voltage Alternating Current Direct Current
p.u.	per unit
PCC	Point of Common Coupling
PV	Photovoltaics
PWM	Pulse Width Modulation
WP	Work Package

Executive Summary

For the implementation of the DC microgrid part of the Italian demonstration in particular a Low Voltage Alternating Current (LVAC) to Direct Current (DC) Active Front End (AFE) is required. Therefore, within HYPERRIDE a bidirectional 34.5 kVA Alternating Current and Direct Current (ACDC) power electronics converter unit from AIT has been used as a basis to implement control algorithms to serve as an AFE and to supply DC microgrids from LVAC power lines. The bidirectional topology enables further to provide power flow towards the DC grid as well as to remove excess generation when a surplus of energy is available.

The developed droop control uses the voltage of the Point of Common Coupling (PCC) as a parameter to control the delivered power. Within the respective task, the control algorithm has been defined, tested and validated in a Controller Hardware-in-the-loop (C-HIL) environment.

In a subsequent step, the unit has been set up as real hardware to test the control algorithm. Successful tests were carried out in the AIT laboratory premises and results are reported in this document.

1 Introduction

1.1 Purpose and Scope of the Document

This report describes and concludes the activities of Task 3.12 “Control Algorithms Implementation for a LVACDC Active Frontend” as stated in the Description of Action (DoA)). For the implementation of the DC microgrid part of the Italian demonstration in particular a functional LVAC to DC AFE is required. Therefore, the controls development has been carried out at and by the HYPERRIDE partner AIT Austrian Institute of Technology and was implemented and validated on the AIT’s power electronics converter system AIT Smart Grid Converter (ASGC). As the AIT’s ASGC was designed to interface Photovoltaics (PV), Battery Energy Storage (BES) and/or Electric Vehicle (EV) to a power grid, additional functionalities were to be implemented in or to provide support for DC µGrids. Here, it was also possible to lever on knowledge from previous DC projects. The laboratory demonstration of these operation modes have been defined as the respective Deliverable D3.12, while this report was defined to collect the most important findings with respect to the demonstration. It should be noted that the controls developed under this project can be employed on other 3-phase active front end bidirectional power converters, hence the implementation is not platform specific and it’s rather generic and portable.

1.2 Structure of the Document

This document is organised as follows: Section 2 introduces the ASGC as an AFE. This includes a presentation of the converter system with specification as well as a principle description of the necessary droop control to provide grid support, Section 3 presents the preceding C-HIL setup for virtual controls development and the laboratory setup to validate the converter system with real power flow, Section 4 describes the most relevant test cases and presents the respective measurement results to proof the correct implementation. Finally, the deliverable is concluded in Section 5.

2 AIT Smart Grid Converter as Active Front End

The ASGC is a four quadrant 35 kVA four phase power converter suitable for a range of Smart Grid applications, such as: grid connected PV or battery storage converter, grid connected currents balancer, active harmonics filter, grid forming converter and active front end.

Having the 4th phase, the ASGC is capable of handling unbalanced voltage and load imbalances found in low voltage Alternating Current (AC) 3-phase and 4-wire grid, micro-grid and hybrid grid applications. For the Hyperride project, the ASGC is configured as a bidirectional AC/DC 3-phase 4-wire power converter or AFE featuring a DC droop control. The DC droop control enables power sharing among AFEs, as well as bidirectional power flow between AC and DC hybrid grids.

The ASGC is a flexible power conversion AC/DC or DC/AC 3-phase 4-wire platform designed as a building block for various applications, such as laboratory setups, field trials and other research projects.

Figure 1: Exterior view of the AIT Smart Grid Converter.

2.1 Droop Control

One important aspect of multiple converters supplying a microgrid is the controllable load sharing between those grid components. One approach to achieve that requirement is the method of droop control by implementing a droop curve which enables control actions by the individual converter based on grid parameters accessible at the PCC. This method has been already implemented with LVAC grids using P-ω/Q-V curves (Hou et al., 2016). Naturally, this approach has been proposed for DC-grids as well. The benefits are the mere independence of the converters from each other, thus keeping the system setup rather simple while enabling easy plug and play extension of grids (Liu, Han, Lin, Yang, & Wang, 2019). A detailed review of DC microgrid control strategies can be found with e.g. (Meng et al., 2017).

Figure 2 shows a block diagram of the DC droop control that has been implemented on the AIT Smart Grid Converter.

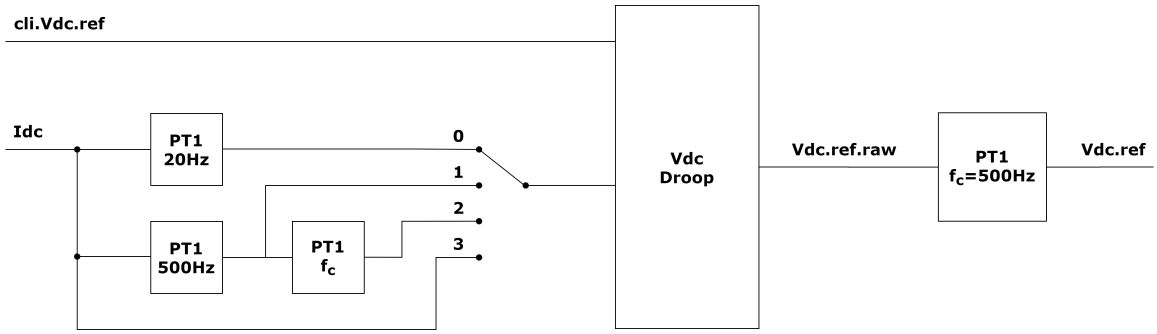

Figure 2: Block diagram of the DC droop control.

Parameter cli.Vdc.ref is set by the user over the Command Line Interface (CLI) and provides a reference setpoint for the DC bus voltage. When the DC droop control is active, it takes cli.Vdc.ref as a base and depending on the current measured on the DC bus (Idc) calculates the value of parameter Vdc.ref which is used as an internal reference value for the DC voltage.

Depending on the selected mode, DC droop control uses different values of the measured current signal Idc:

- 0: Idc filtered at a cutoff frequency of 20 Hz,
- 1: Idc filtered at a cutoff frequency of 500 Hz,
- 2: Idc filtered at a cutoff frequency set by the user and derived from the Idc signal filtered at 500 Hz, and
- 3: unfiltered Idc signal.

The DC droop function is a linear function and it behaves according to the following relation:

$$Vdc.ref = cli.Vdc.ref - Idc * Vdc.droop.factor \quad (1)$$

It results in a DC voltage reference signal which is then filtered at a cutoff frequency which is either set by the user or the default value of 500 Hz is used.

Droop factor is implemented using the p.u. values of DC voltage and DC current. It is preset to 2 % but can easily be changed by the user even during operation. A droop factor of 2 % means that when the DC current is at its nominal value of 60 A, it will cause a DC voltage drop or DC voltage increase (depending on the direction of the power flow) of 2 % of the nominal voltage value which is 1000 V. In the case when AFE is delivering the power to the DC uGrid voltage will decrease depending on the DC current and the droop factor, and in the case when AFE is feeding back the power into the AC grid DC voltage will increase based on the DC current and the droop factor.

The general approach in implementation was to provide flexibility of changing droop curves individually and even during operation. An example of such curves for two AFE can be seen in Figure 3.

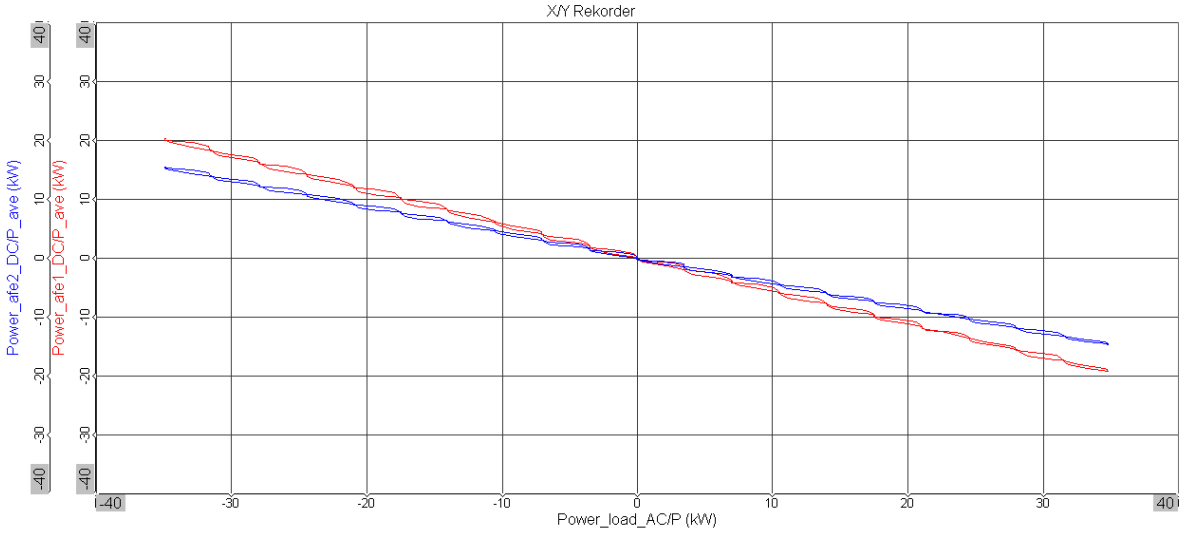

Figure 3: Exemplary XY plot of the implemented AFE droop curves.

2.2 Specification

As a basis for the implementation of an AFE control strategy for DC µGrids a converter system is used, which has been developed at AIT in previous projects. The topology for this 34.5 kVA converter is a 3-Level T-type converter with 4 wires on AC side and 3 wire DC connection. This enables both DC droop control and AC support functions for power quality improvement. The ASGC does not feature internal galvanic separation, which has to be provided by external means (e.g., isolation transformer). A detailed specification of the converter system can be found in Table 1.

Table 1: Specification of AIT Smart Grid Converter Active Front End implementation.

	values	unit
Power		
Power rating	34.5	kW
DC side		
DC nominal input voltage	700	V
DC max. input voltage	1000	V
DC operating voltage range at nominal AC voltage	570 - 950	V
DC (full power) voltage range (PF=1)	570 - 850	V
DC max. short circuit current	75	A
DC max. operating current	60	A
AC side		
AC nominal output voltage	3 NPE 380 / 220V or 3 NPE 400 / 230 or 3 NPE 480/277	V
AC operating voltage range	$\pm$ 20	percent
AC nominal frequency / Frequency range	50 (45-55) or 60 (55-65)	Hz
AC max. continuous output current	50	A
AC output current surge capability	105	A
Power factor range	0 - 1.0	over/under excited
THD at max. power	< 3	percent
General data		
Peak efficiency / Weighted efficiency EU/CEC	> 98	percent
Enclosure type protection class (electronics/mags)	IP54/IP20	
Ambient air temperature for operation	-25 to +60	degC
Relative humidity	0 - 100	percent (non-condensing)
Audible noise	35 $\pm$ 3	dBA
Other		
Communications	ModBus TCP, IEC61850	
Safety and EMC	IEC 62477-1, IEC 62109, IEC 61000-6-2, IEC 61000-6-3	
Grid code compliance (examples)	VDE-AR-N4110, VDE-AR-N4105, IEEE1547-2018	

3 Test setup

To test and validate the control strategy implemented in the converter system two steps have been taken. Firstly, the basic functions were tested in a virtual C-HIL environment and after the integration of the full control algorithms the controller firmware has been transferred to a real power converter which has been tested in a laboratory infrastructure. Both validation steps are described with exemplary results in the two subsequent sections.

3.1 C-HIL setup

Controller hardware-in-the-loop (C-HIL) is a type of real-time simulation in which the real hardware controller is interfaced with the simulation of the power system. C-HIL is an effective way of testing the controls since it provides insight into the real time behaviour with signals shown in high fidelity. For the validation of DC droop control, simulation step of 2 ns was used.

The C-HIL setup in Figure 4 consists of two Typhoon HIL 602+ emulators connected in parallel and one AIT HIL Controller connected to each Typhoon HIL device.

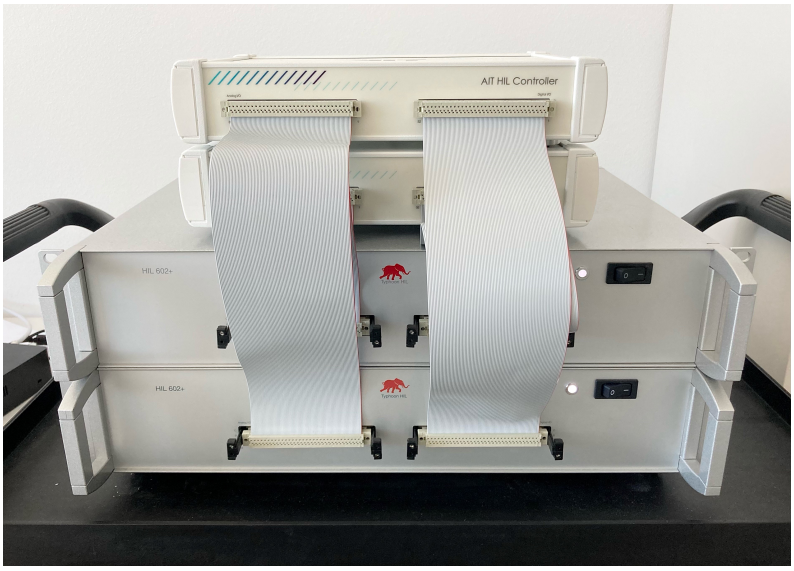

Figure 4: C-HIL setup with two Typhoon HIL 602+ emulators and two AIT HIL Controllers.

AIT HIL Controller was developed as a digital twin to ASGC and inside each device is the exact same control board with the same firmware running on it. The controller was also designed to easily interface with the Typhoon HIL emulator. In this setup, AIT HIL Controller carries out the converter control including the DC droop control while all the other components of the µGrid, i.e. electrical grid, transformer, pre-charge circuit, converter power train are simulated inside Typhoon HIL 602+ emulator.

Simulation model shown in Figure 5 consists of two ASGCs, named AFE1 and AFE2, each connected on the AC side through a transformer to a common AC grid and on the DC side to a shared DC load. Due to a limited number of available processing cores on each Typhoon HIL 602+ device it was not possible to simulate another ASGC as a DC load. Such model would require more processing power due to its complexity. Instead, a constant current source was used. Between each AFE and the DC load, there is an impedance which was simulated using

an RL section component from the standard Typhoon HIL library. RL section is a simplified model of a transmission line. It is defined by three parameters: per length resistance, per length inductance and cable length. In this model, impedance values measured in the laboratory were used. SGC component is not part of the standard Typhoon HIL library, but it is a user defined component and represents a model of ASGC's power stage. Its nominal power, nominal current and nominal grid voltage can be set by the user. Internal structure of the component can't be accessed, but the component consists of a DC bus, a switching bridge, an AC filter and an AC relay to the grid which are all simulated inside Typhoon HIL emulator. Pulse Width Modulation (PWM) signals and relay control signals on the other hand are not simulated and are coming directly from the controller.

As mentioned previously, each Typhoon HIL device has a limited number of processing cores. That is why two devices connected in parallel had to be used. AFE1, its transformer, grid simulator, pre-charge circuit and DC impedance and DC load are simulated in one Typhoon HIL 602+ device while DC2 and its transformer are simulated in the other device.

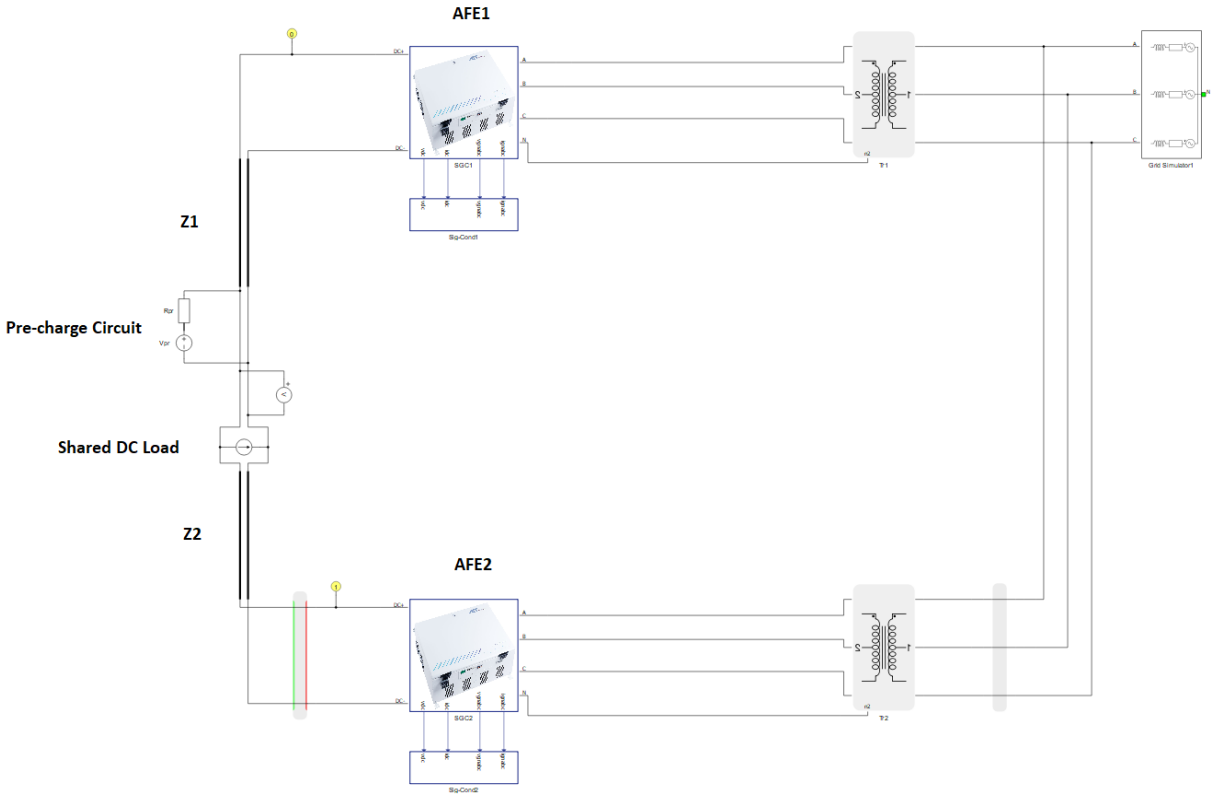

Figure 5: Simulation model for Active Front End validation.

A number of different test cases like the ones performed in the laboratory were first executed on the C-HIL setup to ensure proper functionality of the system and to avoid unwanted overloads and trips once the actual converter is put into use.

C-HIL simulation was also used to fine tune DC droop parameters and to determine droop factor of the two AFEs in order for them to share the DC load equally. Simulation showed that when AFE2 droop factor is set to 1 %, droop factor of AFE1 should be set to 1.8 %.

Below are the test results for the case when both AFEs are running at full power and then AFE1 is powered off and powered on again. Test case parameters are give in the Table 2.

Table 2: Parameters for the test case when AFE1 is powered off.

Parameter	Value	Unit
P_{AFE1}	0	p.u.
$Droop_{AFE1}$	1.8	%
P_{AFE2}	1	p.u.
$Droop_{AFE2}$	1	%
I_{LOAD}	40	A
$V_{DC,ref}$	700	V

Figure 6 shows DC voltage, current and power of AFE1 and AFE2 when AFE1 is powered off. Figure 7 shows DC voltage, current and power of AFE1 and AFE2 when AFE1 is powered on.

Figure 8 shows the transient response of DC voltage and current of AFE1 and AFE2 when AFE1 is powered off. Figure 9 shows transient response of DC voltage and current of AFE1 and AFE2 when AFE1 is powered on.

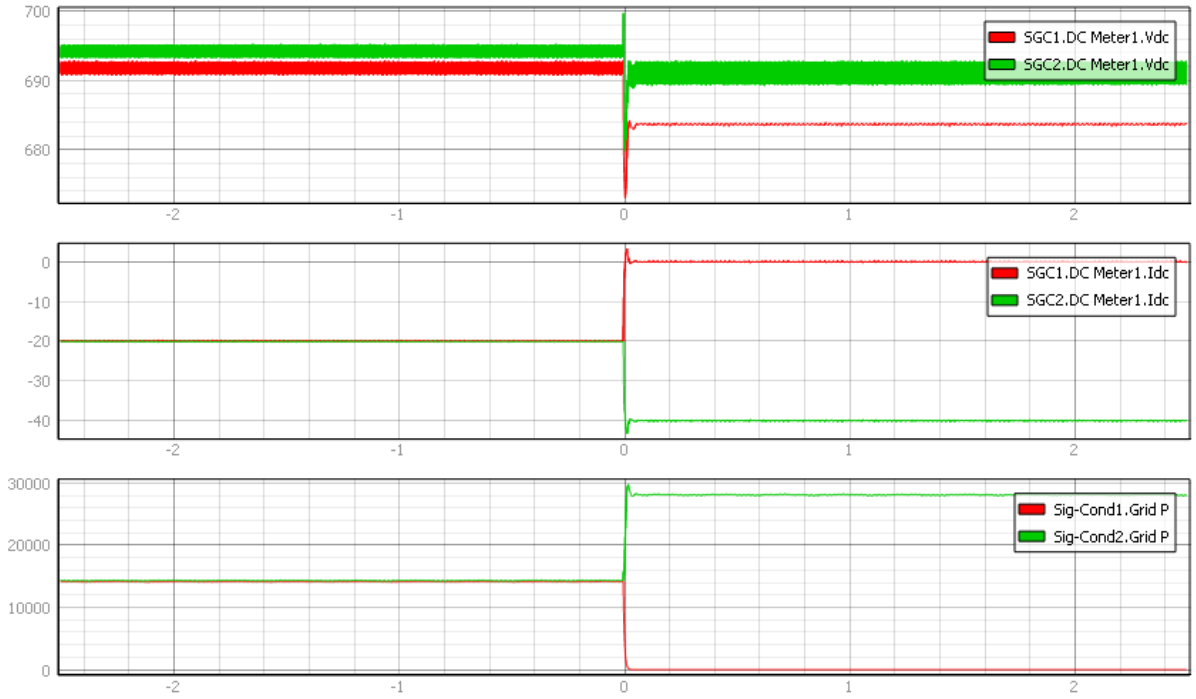

Figure 6: DC voltage, current and power when AFE1 is turned off.

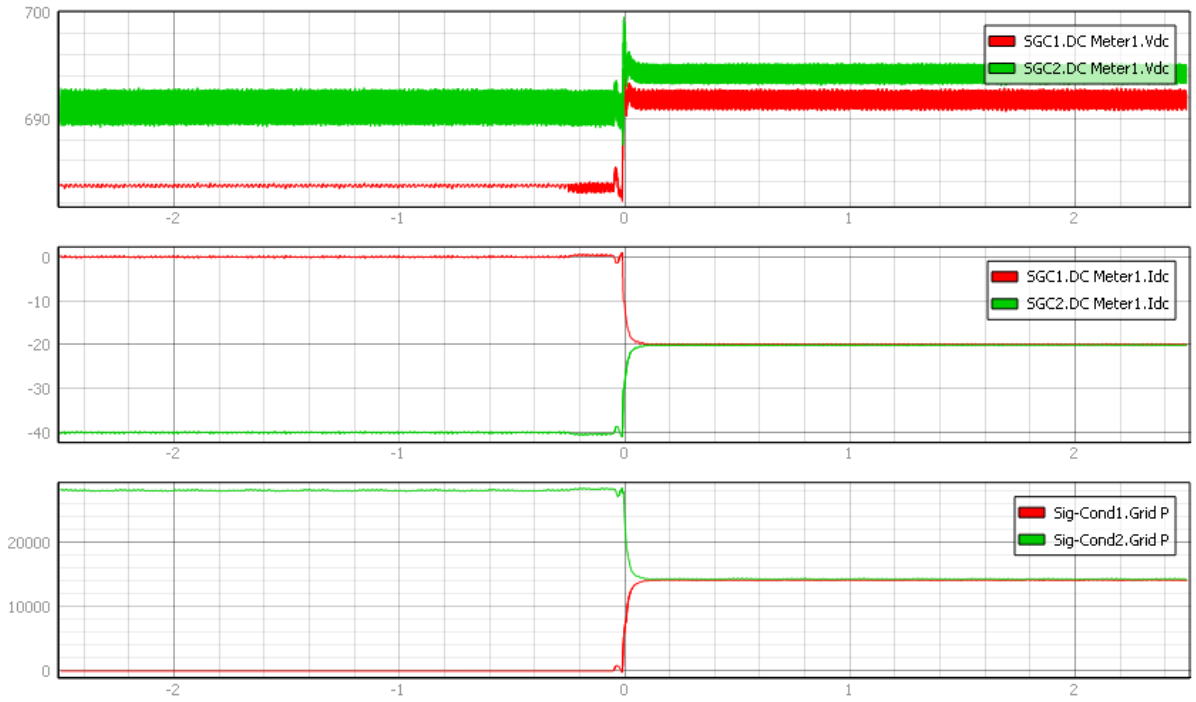

Figure 7: DC voltage, current and power when AFE1 is turned on.

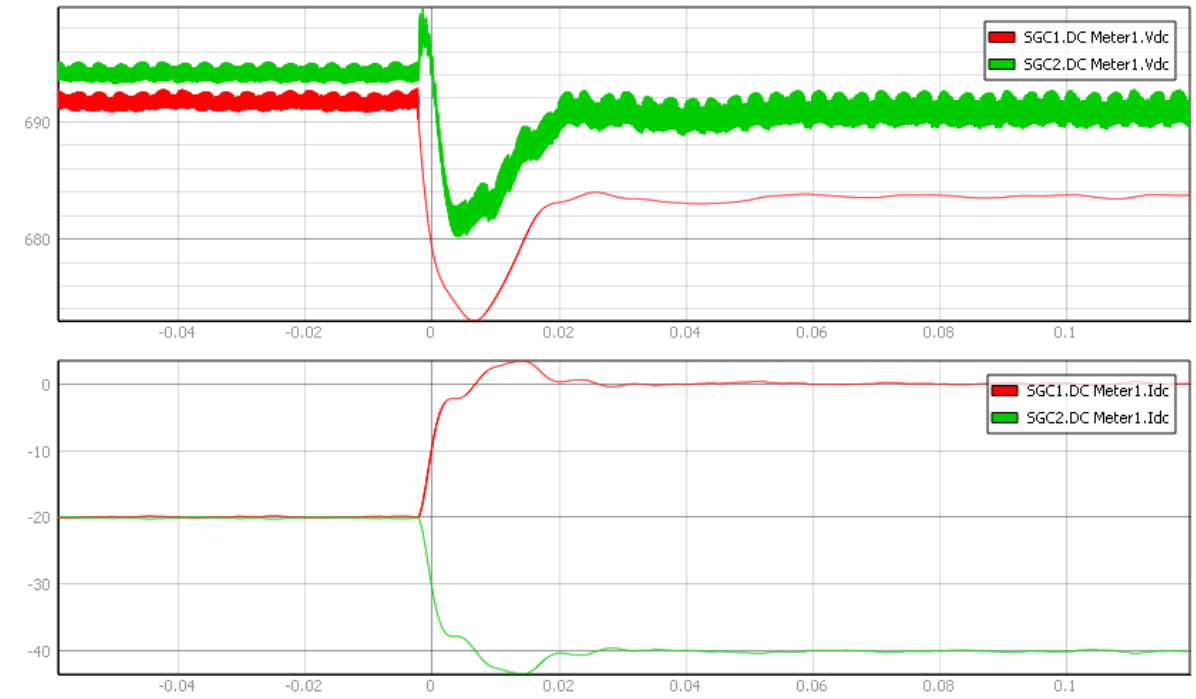

Figure 8: Transient response of DC voltage and current when AFE1 is turned off.

doi:10.5281/zenodo.5115844

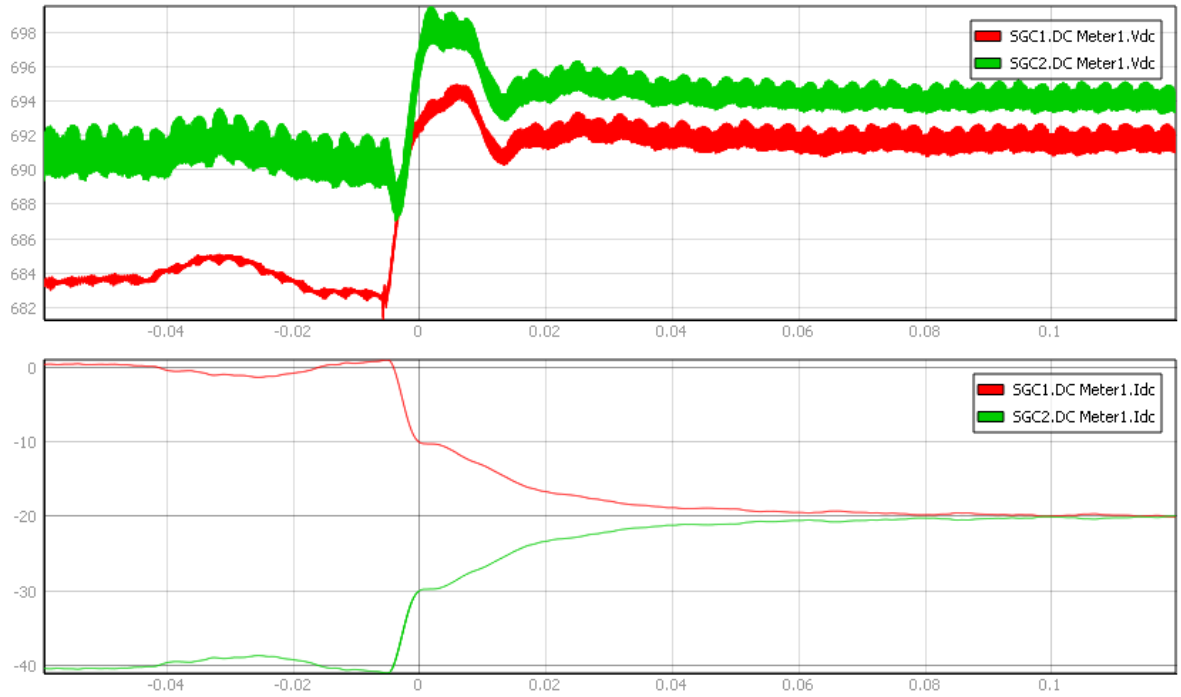

Figure 9: Transient response of DC voltage and current when AFE1 is turned on.

3.2 Laboratory setup

The laboratory setup consists of two ASGCs working in AFE mode, designated AFE1 and AFE2, their respective transformers and one ASGC acting as a load. As shown in Figure 10, the two AFEs supply the load on the DC line while the load feeds the power back to the the common AC grid. Two defined impedances, Z1 and Z2, are included within the setup to allow for the validation of the implemented droop control. Table 3 provides the values of these impedances.

DC measurements (current and voltage) are implemented on AFE1 as well as AFE2. AC measurements (currents and voltages) are implemented on AFE2 as well as the load. All the measurements are filtered by a butterworth filter at a limiting frequency of 10kHz, reducing the visible crosstalk induced by the switching frequency. While this allows for clean captures it must be noted that measurements of transient responses can be inaccurate.

Figure 11 depicts part of the setup, two ASGCs in a back to back setup, one acting as AFE1, the other as the load.

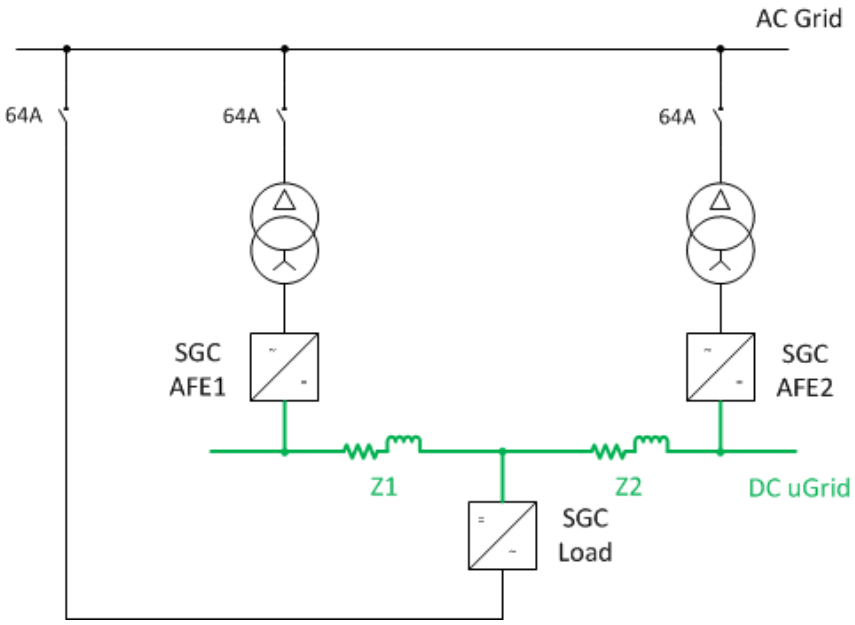

Figure 10: Schematic test setup for Active Front End validation.

Table 3: Values of the DC line impedances.

Designation	Resistance	Inductance
Z1	60 mΩ	0.048 mH
Z2	180 mΩ	1.86 mH

Figure 11: Laboratory setup with two AIT Smart Grid Converters in a back to back setup.

4 Test cases and measurement results

This section presents the results collected during the test execution that assessed device capability under the following conditions: Bidirectional power flow, load sharing, droop adjustment, power surplus/deficit adjustment and power off load transfer.

4.1 Bidirectional power flow

This test case validates bidirectional power flow capabilities of the implemented control algorithms. As summarised in Table 4, AFE1 is inactive, while AFE2 takes the full load. The droop factor is set to 2 % and the DC reference-voltage is set to 700 V.

During the test sequence outlined in Table 5, the power level of the ASGC acting as a load, P_{LOAD}, is first increased towards P_{LOAD} = 0.8 per unit (p.u.), then decreased towards P_{LOAD} = -0.8 p.u. in increments of +/- 0.1 p.u., showing power flow in both directions.

Figure 12 provides an overview over the DC power levels, while Figure 13 shows DC voltages and currents of AFE1 and AFE2. Figure 14 depicts the XY-plot of the AFEs' DC voltages over currents, providing a visualisation of the implemented droop factor of 2 % p.u., amounting to the expected 0.333 V/A. Figure 15 shows AFE DC power levels over load AC power.

Due to high impedances on the AC line it was not feasible to go to a higher power level, as this would have resulted in the AFE entering AC current derating mode. This is an important finding as it might suggest using transformers with multiple taps in WP08 to be able to adjust AC input-voltage levels according to AC line impedances.

Table 4: Parameters for the test case validating bidirectional power flow.

Parameter	Value	Unit
$P_{MAXAFE1}$	0	p.u.
$Droop_{AFE1}$	2	%
$P_{MAXAFE2}$	1	p.u.
$Droop_{AFE2}$	2	%
$V_{DC,ref}$	700	V

Table 5: Test Sequence for the test case validating bidirectional power flow.

Test time	Parameter	Change
t_0	P_{LOAD}	0 p.u.
$t_0 \rightarrow t_1$	P_{LOAD}	stepwise increase
t_1	P_{LOAD}	0.8 p.u.
$t_1 \rightarrow t_2$	P_{LOAD}	stepwise decrease
t_2	P_{LOAD}	-0.8 p.u.
$t_2 \rightarrow t_3$	P_{LOAD}	stepwise increase
t_3	P_{LOAD}	0 p.u.

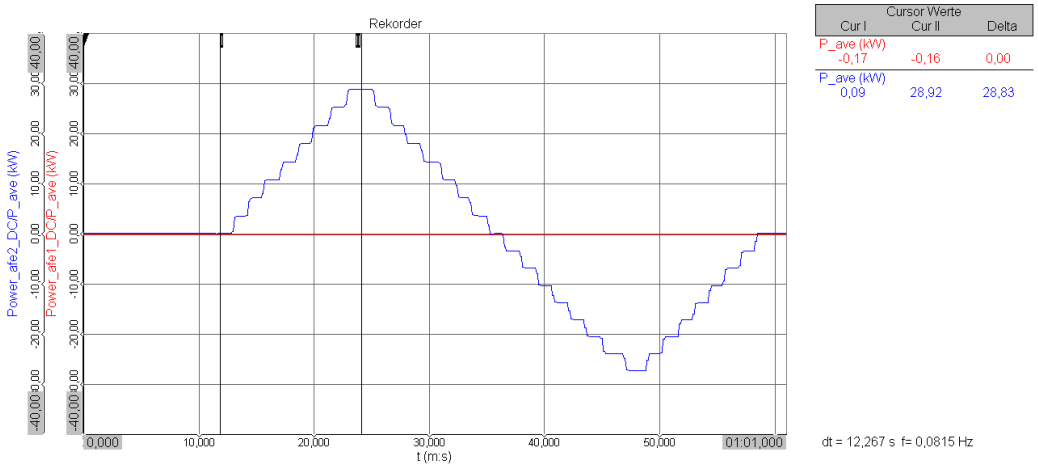

Figure 12: DC power during the bidirectional power flow test case.

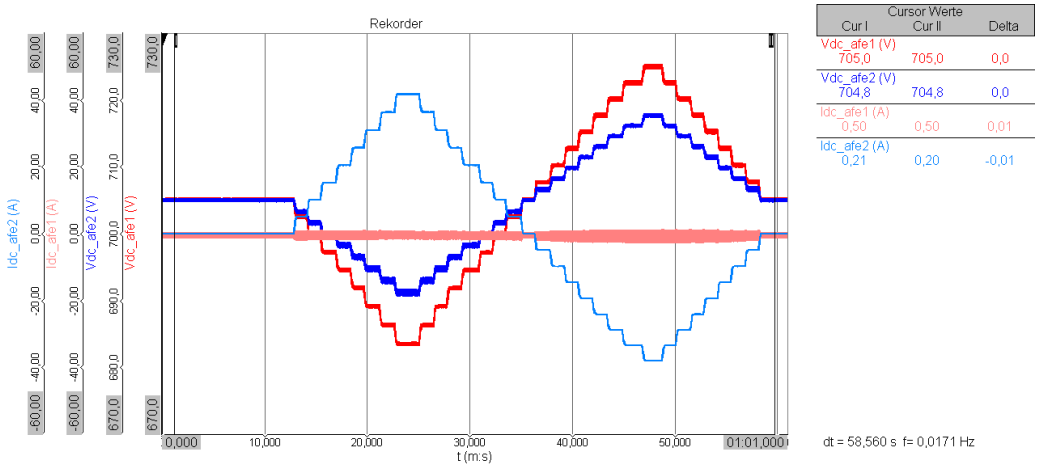

Figure 13: DC voltages and currents during the bidirectional power flow test case.

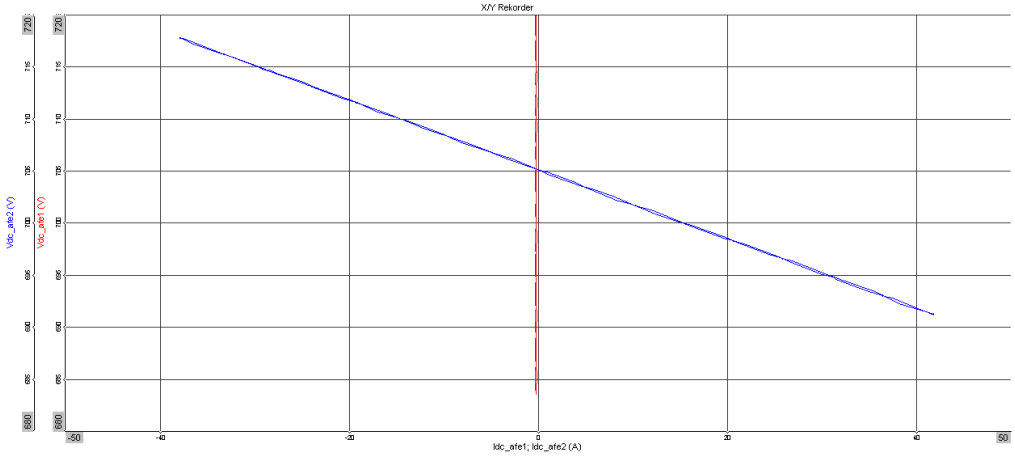

Figure 14: XY-plot of the DC voltages over currents during the bidirectional power flow test case.

 doi:10.5281/zenodo.5115844

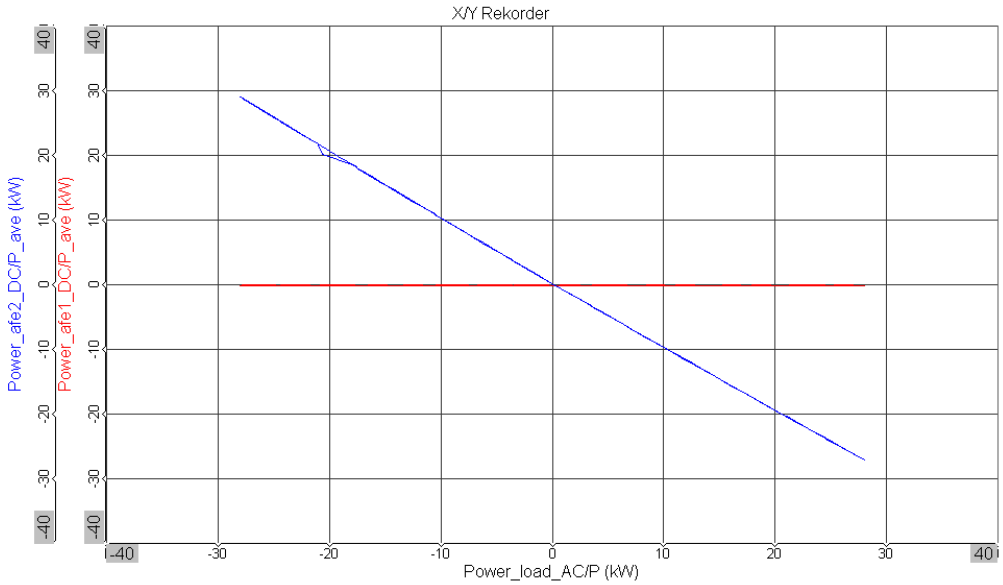

Figure 15: XY-plot of AFE DC power over load AC power during the bidirectional power flow test case.

4.2 Load sharing

This test case validates load sharing capabilities of the implemented control algorithms. As summarised in Table 6, both AFE1 and AFE2 are active, sharing the load. The droop factor of both AFEs is set to 2 % and the DC reference-voltage remains at 700 V.

During the test sequence outlined in Table 7, the power level of the ASGC acting as a load, P_{LOAD}, is first increased towards P_{LOAD} = 1 p.u. then decreased towards P_{LOAD} = -1 p.u. in increments of +/- 0.1 p.u., showing power flow in both directions.

Figure 16 provides an overview over the DC power levels, while Figure 17 shows DC voltages and currents of AFE1 and AFE2. Figure 18 depicts the XY-plot of the AFEs' DC voltages over currents, providing a visualisation of the implemented droop factor of 2 % p.u. Figure 19 shows AFE DC power levels over load AC power.

As expected Figure 18 shows the uniform droop factor of 2 % on both AFEs. As a result of the non-identical DC line impedances the power levels of the two AFEs differ.

Figure 20 shows an oscilloscope plot of the AFEs DC voltages and currents at P_{LOAD}= 1 p.u. The highest voltage ripple can be seen on V_{DCAFE1} amounting to 0.8 V_{P-P}, while the highest current ripple can be seen on I_{DCAFE1} amounting to 2.6 A_{P-P}, sharing the frequency of 285Hz.

Table 6: Parameters for the test case validating load sharing capabilities.

Parameter	Value	Unit
$P_{MAXAFE1}$	1	p.u.
$Droop_{AFE1}$	2	%
$P_{MAXAFE2}$	1	p.u.
$Droop_{AFE2}$	2	%
$V_{DC,ref}$	700	V

doi:10.5281/zenodo.5115844

Table 7: Test Sequence for the test case validating load sharing capabilities.

Test time	Parameter	Change
t_0	P_{LOAD}	0 p.u.
$t_0 \rightarrow t_1$	P_{LOAD}	stepwise increase
t_1	P_{LOAD}	1 p.u.
$t_1 \rightarrow t_2$	P_{LOAD}	stepwise decrease
t_2	P_{LOAD}	-1 p.u.
$t_2 \rightarrow t_3$	P_{LOAD}	stepwise increase
t_3	P_{LOAD}	0 p.u.

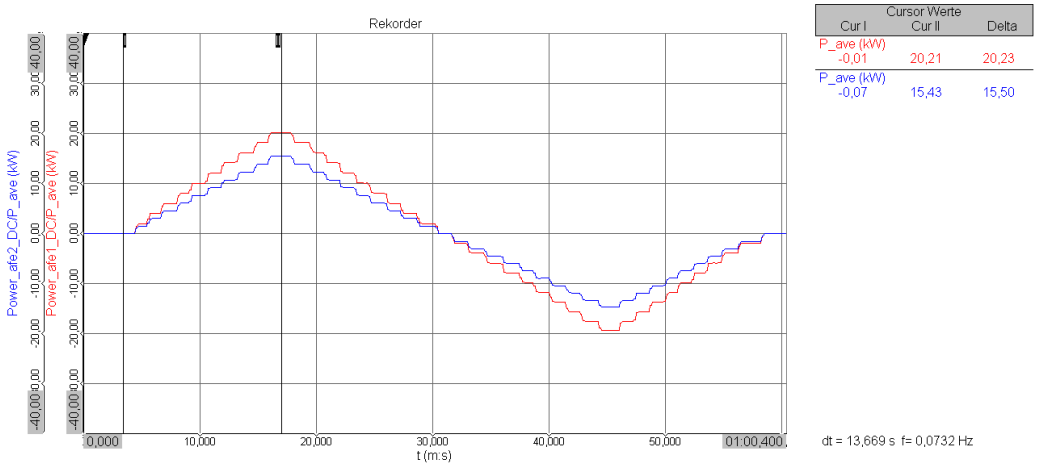

Figure 16: DC power during the load sharing test case.

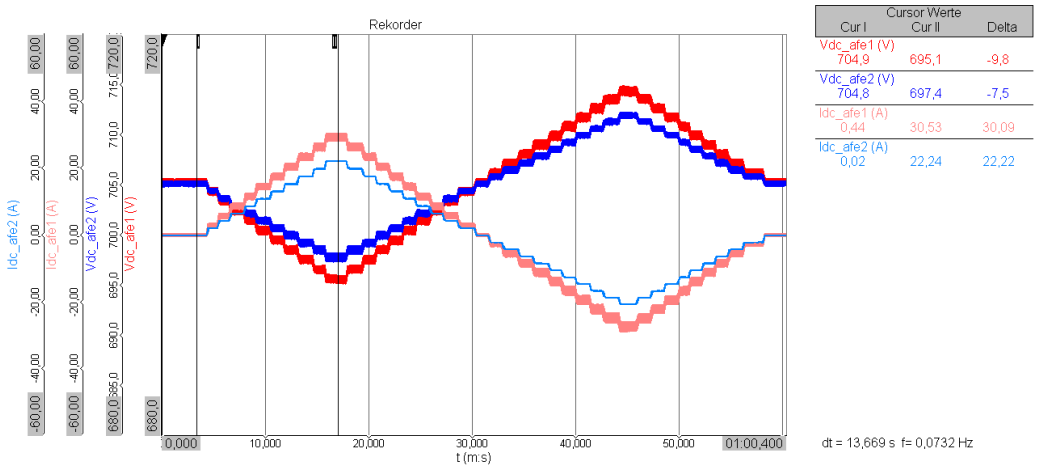

Figure 17: DC voltages and currents during the load sharing test case.

doi:10.5281/zenodo.5115844

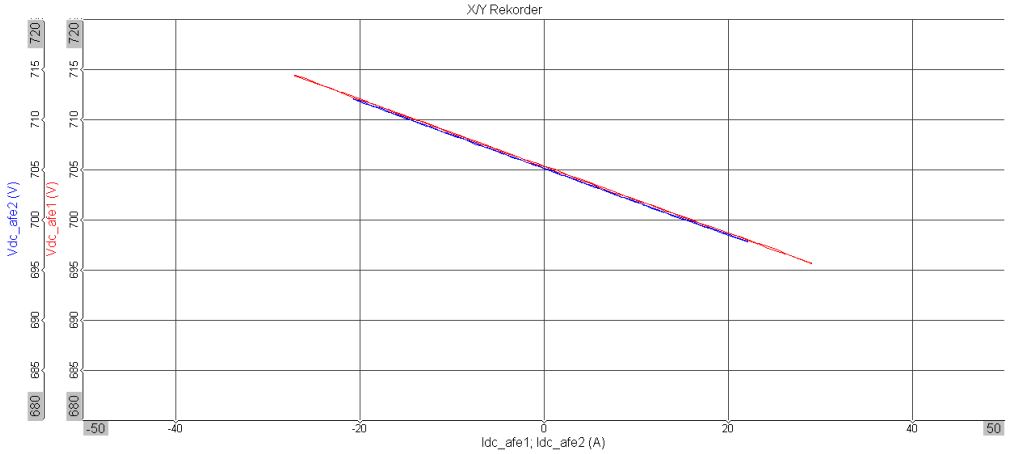

Figure 18: XY-plot of the DC voltages over currents during the load sharing test case.

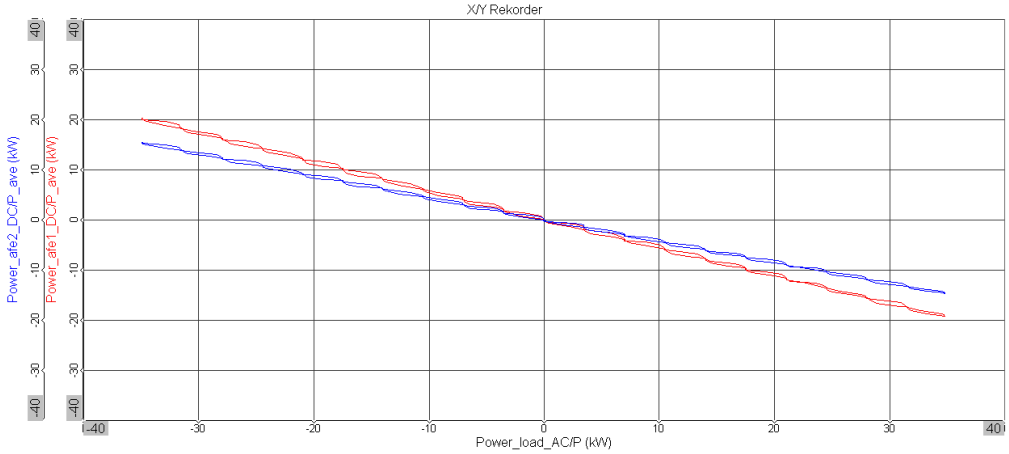

Figure 19: XY-plot of AFE DC power over load AC power during the load sharing test case.

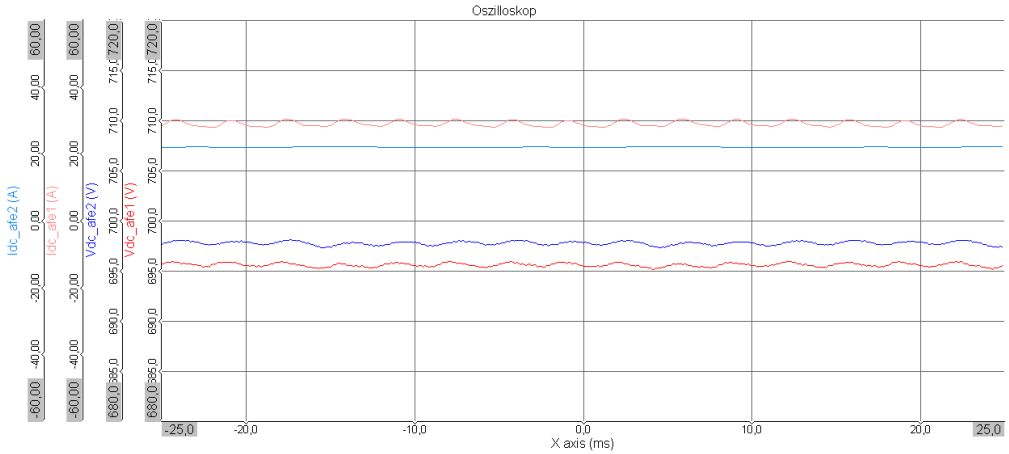

Figure 20: Oscilloscope plot of the DC voltages and currents at P_{LOAD}= 1 p.u. during the load sharing test case.

 doi:10.5281/zenodo.5115844

4.3 Droop adjustment

This test case validates the capabilities of the implemented control algorithms to adjust the droop factor under load and reach uniform load distribution. As summarised in Table 8, both AFE1 and AFE2 are active, sharing the load. The initial droop factor is set to 1 % on both of the AFEs.

During the test sequence outlined in Table 9, the power level of the ASGC acting as a load, P_{LOAD}, is first increased towards P_{LOAD} = 1 p.u. Subsequently the droop factor of AFE1 is increased to 1.76 %, leading to uniform load sharing. Then P_{LOAD} is decreased towards P_{LOAD} = -1 p.u. in increments of -0.1 p.u., showing uniform load sharing both generating as well as sinking power.

Figure 21 provides an overview over the DC power levels, while Figure 22 shows DC voltages and currents of AFE1 and AFE2. Figure 23 depicts the XY-plot of the AFEs' DC voltages over currents, providing a visualisation of the adjustment of the droop factor. Figure 24 shows AFE DC power levels over load AC power.

As expected, at startup, Figure 23 shows the uniform droop factor of 1 %, while Figure 24 shows a deviation in power provided by AFE1 and AFE2. After the adjustment of the droop factor the XY-plots show uniform power sharing and deviating droop values.

Figure 25 shows an oscilloscope plot of the AFEs DC voltages and currents during the transient response of the AFEs during $t_2 \rightarrow t_3$.

Table 8: Parameters for the test case validating droop adjustment under load.

Parameter	Value	Unit
$P_{MAXAFE1}$	1	p.u.
$Droop_{AFE1}$	1	%
$P_{MAXAFE2}$	1	p.u.
$Droop_{AFE2}$	1	%
$V_{DC,ref}$	700	V

Table 9: Test Sequence for the test case validating droop adjustment under load.

Test time	Parameter	Change
t_0	P_{LOAD}	0 p.u.
$t_0 \rightarrow t_1$	P_{LOAD}	stepwise increase
t_1	P_{LOAD}	1 p.u.
t_2	$Droop_{AFE2}$	set to 1.76 %
$t_2 \rightarrow t_3$	P_{AFE1}; P_{AFE2}	transient change
$t_4 \rightarrow t_5$	P_{LOAD}	stepwise decrease
t_5	P_{LOAD}	-1 p.u.
$t_5 \rightarrow t_6$	P_{LOAD}	stepwise increase
t_6	P_{LOAD}	0 p.u.

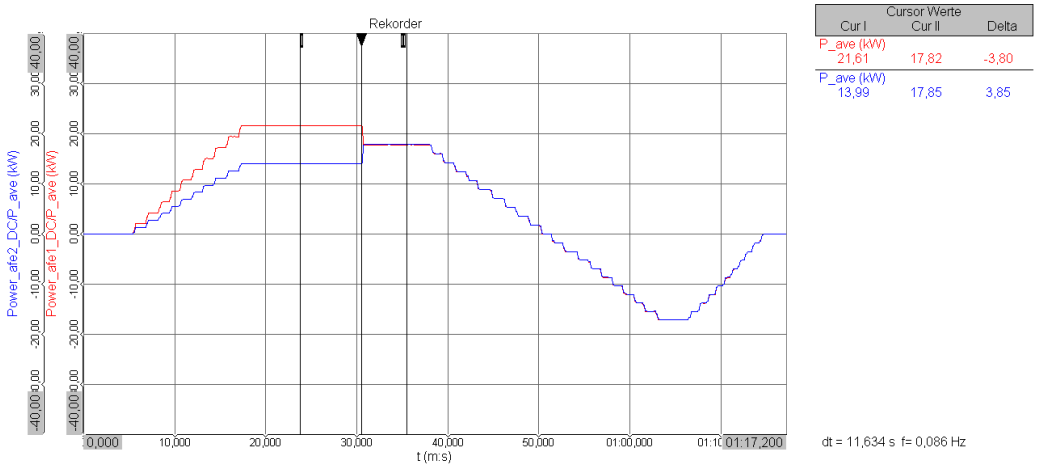

Figure 21: DC power during droop adjustment.

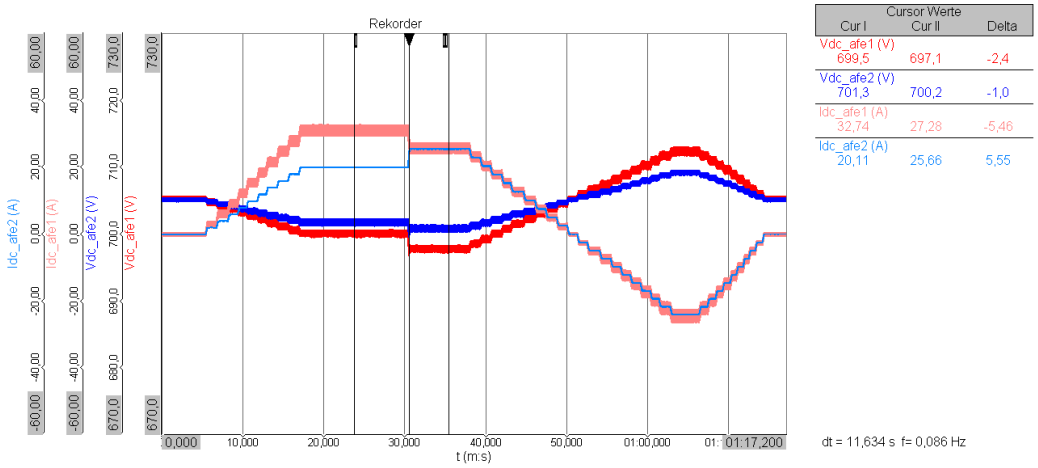

Figure 22: DC voltages and currents during droop adjustment.

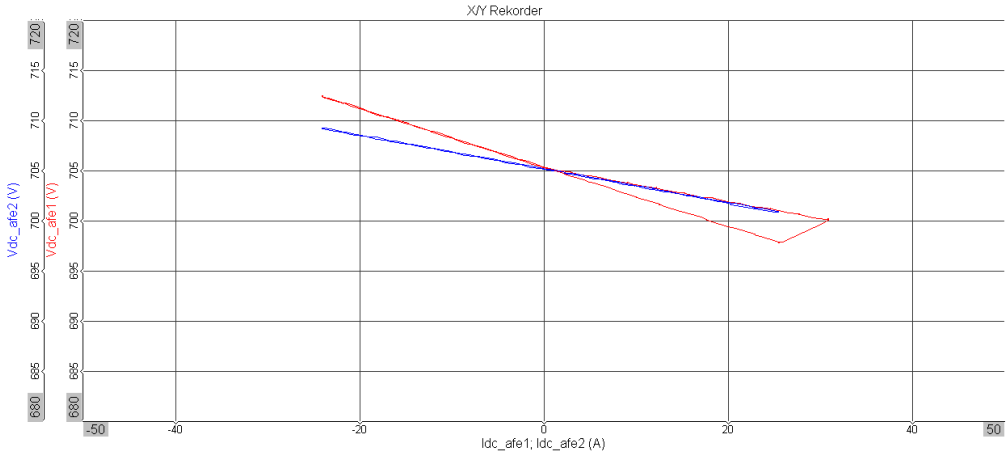

Figure 23: XY-plot of the DC voltages over currents during droop adjustment.

doi:10.5281/zenodo.5115844

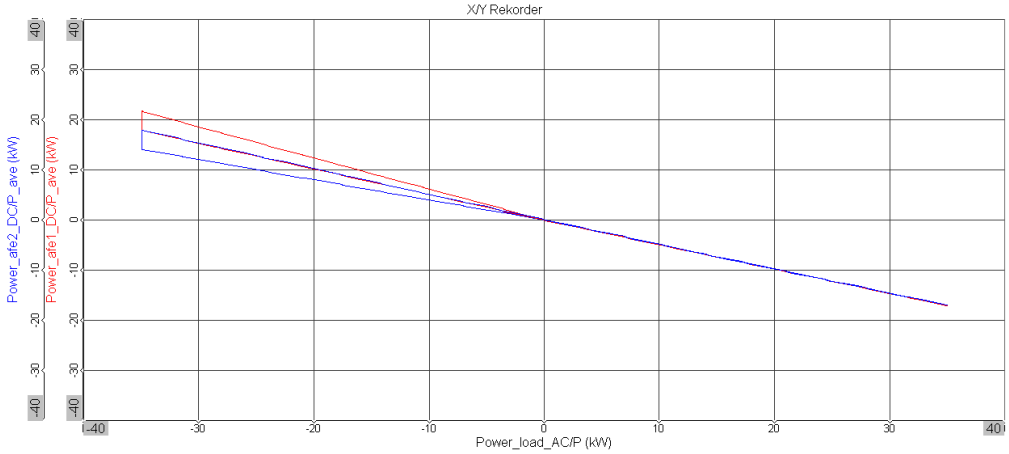

Figure 24: XY-plot of AFE DC power over load AC power during droop adjustment.

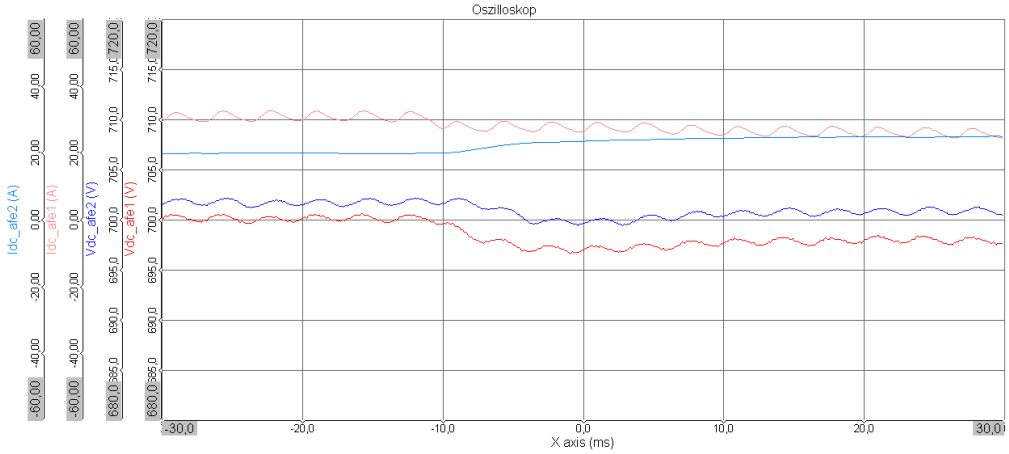

Figure 25: Oscilloscope plot (DC voltages and currents) of the transient response during droop adjustment.

4.4 Power surplus/deficit adjustment

This test case shows the AFEs' behaviour during a transient change of load. As summarised in Table 10, both AFE1 and AFE2 are active, sharing the load. The droop factors remain at the settings used for uniform load sharing.

During the test sequence outlined in Table 11, the power level of the ASGC acting as a load, P_{LOAD}, starting at P_{LOAD} = 0 p.u., is first set to P_{LOAD} = 1 p.u. Subsequently it is set to P_{LOAD} = -1 p.u., returning towards P_{LOAD} = 0 p.u. thereafter.

Figure 26 provides an overview over the DC power levels, while Figure 27 shows DC voltages and currents of AFE1 and AFE2. Figure 28 depicts the XY-plot of the AFEs' DC voltages over currents. Figure 29 shows AFE DC power levels over load AC power.

As expected, Figure 28 shows some deviation from the ideal droop control during the transient response, Figure 29 however shows almost uniform load sharing.

Figure 30 shows an oscilloscope plot of the AFEs DC voltages and currents during the transient

response of the AFEs during $t_2 \rightarrow t_3$.

Table 10: Parameters for the test case exploring power surplus/deficit adjustment.

Parameter	Value	Unit
$P_{MAXAFE1}$	1	p.u.
$Droop_{AFE1}$	1.76	%
$P_{MAXAFE2}$	1	p.u.
$Droop_{AFE2}$	1	%
$V_{DC,ref}$	700	V

Table 11: Test Sequence for the test case exploring power surplus/deficit adjustment.

Test time	Parameter	Change
t_0	P_{LOAD}	0 p.u.
$t_0 \rightarrow t_1$	P_{LOAD}	transient increase
t_1	P_{LOAD}	1 p.u.
$t_2 \rightarrow t_3$	P_{LOAD}	transient decrease
t_3	P_{LOAD}	-1 p.u.
$t_4 \rightarrow t_5$	P_{LOAD}	transient increase
t_5	P_{LOAD}	0 p.u.

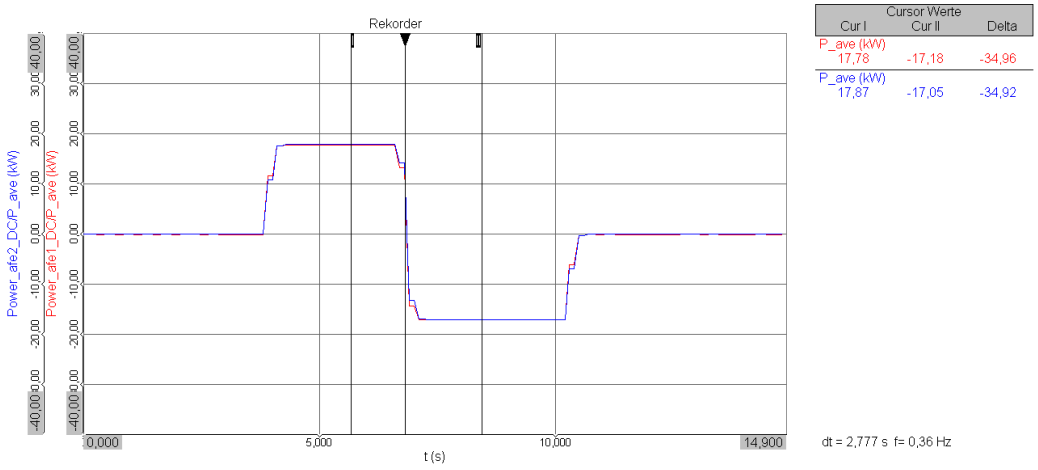

Figure 26: DC power during power surplus/deficit adjustment.

doi:10.5281/zenodo.5115844

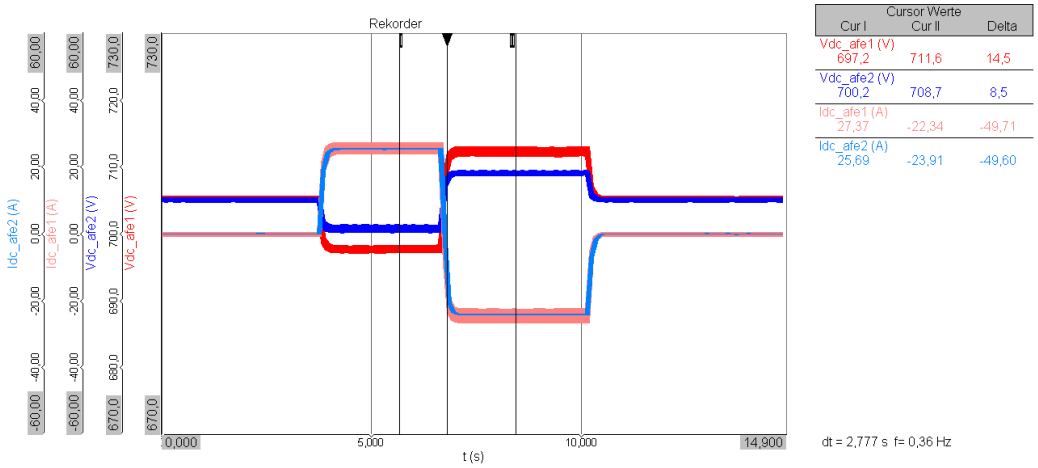

Figure 27: DC voltages and currents during power surplus/deficit adjustment.

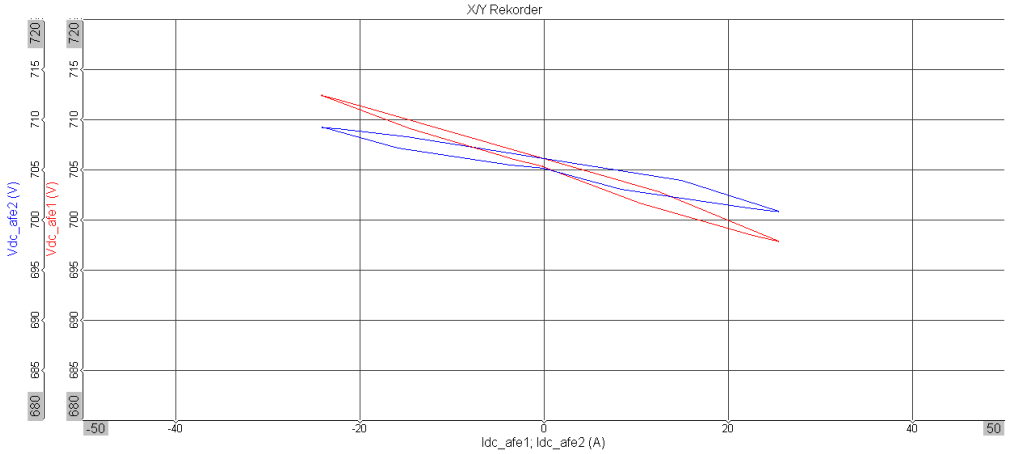

Figure 28: XY-plot of the DC voltages over currents during power surplus/deficit adjustment.

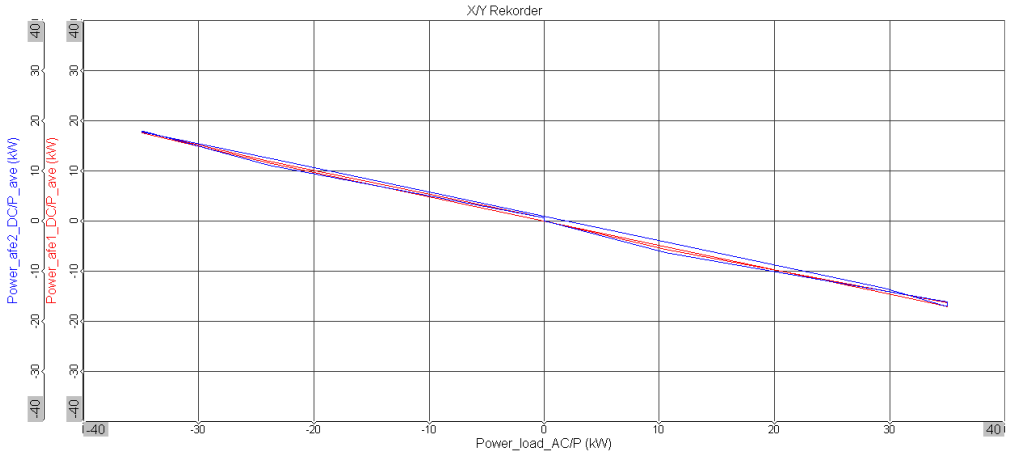

Figure 29: XY-plot of AFE DC power over load AC power during power surplus/deficit adjustment.

doi:10.5281/zenodo.5115844

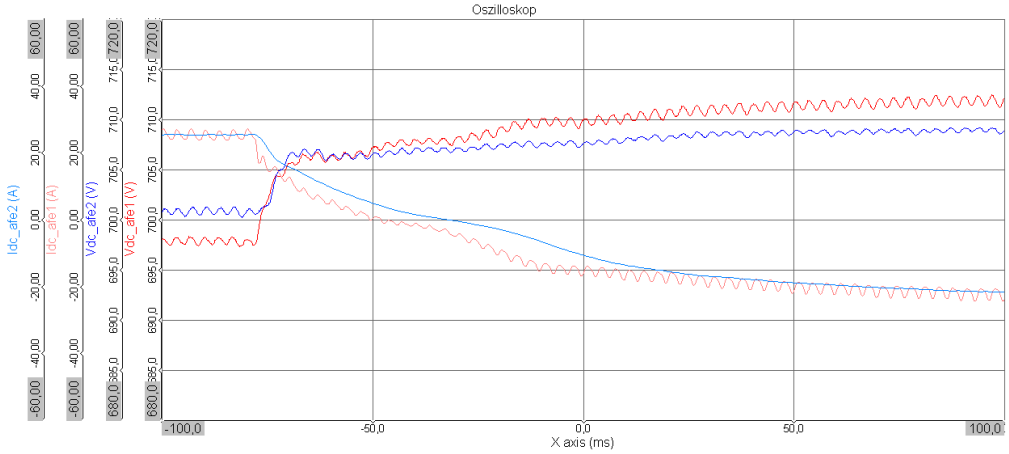

Figure 30: Oscilloscope plot (DC voltages and currents) of the transient response during power surplus/deficit adjustment.

4.5 Power off load transfer

This test case shows the AFEs' behaviour during a load transfer from one AFE to the other initiated by powering one of them on and off subsequently.

During the power off sequence the AFEs' AC relays open. Therefore the AC side is of relevance to this test case. However, as described in Section 3.2 Laboratory setup, AC measurements are only implemented on AFE2. To provide captures of the AC side in both scenarios, the test has been split into two sections. First AFE1 is powered on and off, while AFE2 stays powered on. Afterwards AFE2 is powered on and off, while AFE1 stays powered on.

4.5.1 AFE1 powered on and off

As summarised in Table 12, AFE1 starts in the powered off state, while AFE2 supplies all power demanded by the load, P_{LOAD} = 0.8 p.u. The droop factors remain at the settings used for uniform load sharing.

During the test sequence outlined in Table 13, AFE1 is powered on, followed by a transient response of both AFEs, settling at uniform load sharing. Afterwards AFE1 is powered off.

Figure 31 provides an overview over the DC power levels, while Figure 32 shows DC voltages and currents of AFE1 and AFE2.

The transient responses of the AFEs on the DC side are captured in the oscilloscope plots Figure 33 and Figure 34. The highest voltage-overshoot can be noticed on V_{DCAFE1} during turn-off, amounting to 8.6 V. I_{DCAFE2} shows the highest current overshoot equalling 4.7 A, also during turn-off.

The transient responses on the AC side are captured in the oscilloscope plots Figure 35 and Figure 36. Power-on of AFE1 leads to a clean reduction of AC currents of AFE2. During power-off of AFE1, an overshoot of AFE2s AC-currents can be noticed. It amounts to 9.76 A equalling 16 % of the settled current values.

Table 12: Parameters for the test case exploring the load transfer when AFE1 is powered on and off.

Parameter	Value	Unit
$State_{AFE1}$	OFF	n.a.
$P_{MAXAFE1}$	1	p.u.
$Droop_{AFE1}$	1.76	%
$State_{AFE2}$	ON	n.a.
$P_{MAXAFE2}$	1	p.u.
$Droop_{AFE2}$	1	%
P_{LOAD}	0.8	p.u.
$V_{DC,ref}$	700	V

Table 13: Test Sequence for the test case exploring the load transfer when AFE1 is powered on and off.

Test time	Parameter	Change
t_0	$State_{AFE1}$	OFF
t_0	$State_{AFE2}$	ON
$t_1 \rightarrow t_2$	P_{AFE1}; P_{AFE2}	transient change
t_2	$State_{AFE1}$; $State_{AFE2}$	ON
$t_3 \rightarrow t_4$	P_{AFE1}; P_{AFE2}	transient change
t_4	$State_{AFE1}$	OFF
t_4	$State_{AFE2}$	ON

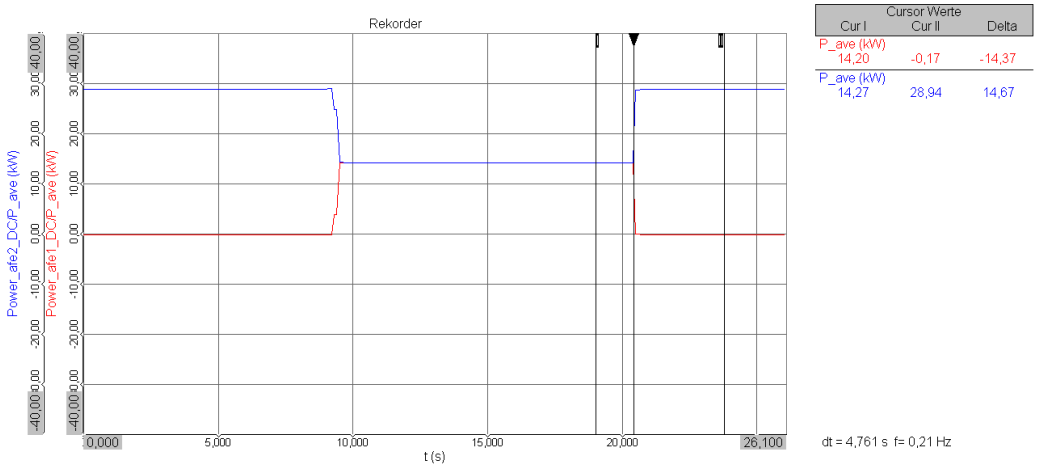

Figure 31: DC power during power off load transfer (AFE1 on/off).

doi:10.5281/zenodo.5115844

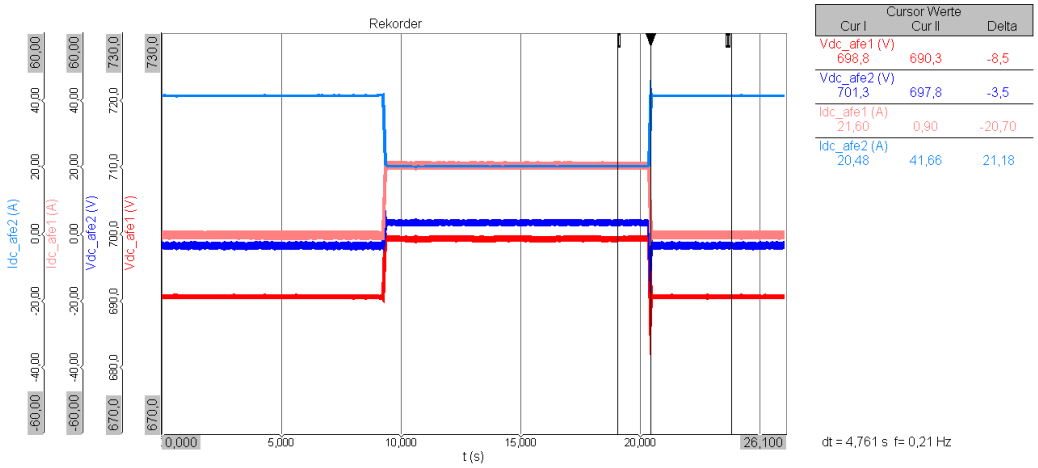

Figure 32: DC voltages and currents during power off load transfer (AFE1 on/off).

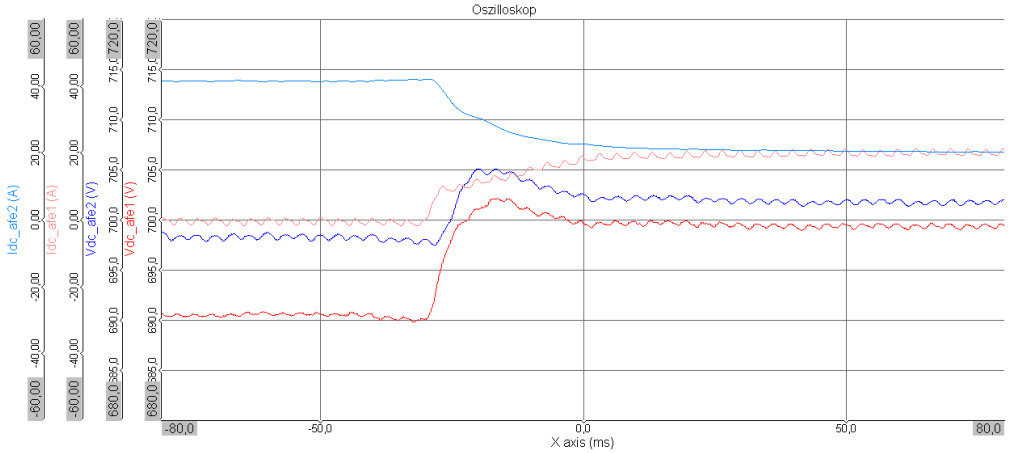

Figure 33: Oscilloscope plot of the DC voltages and currents during the transient load transfer when AFE1 is powered on.

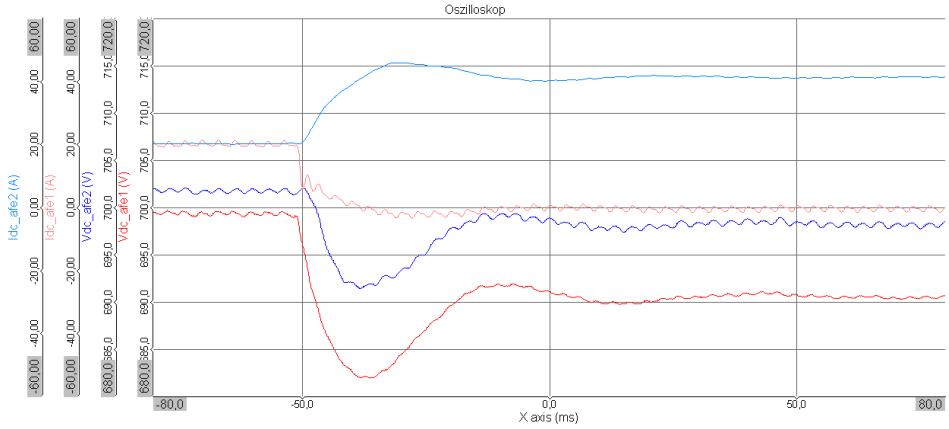

Figure 34: Oscilloscope plot of the DC voltages and currents during the transient load transfer when AFE1 is powered off.

doi:10.5281/zenodo.5115844

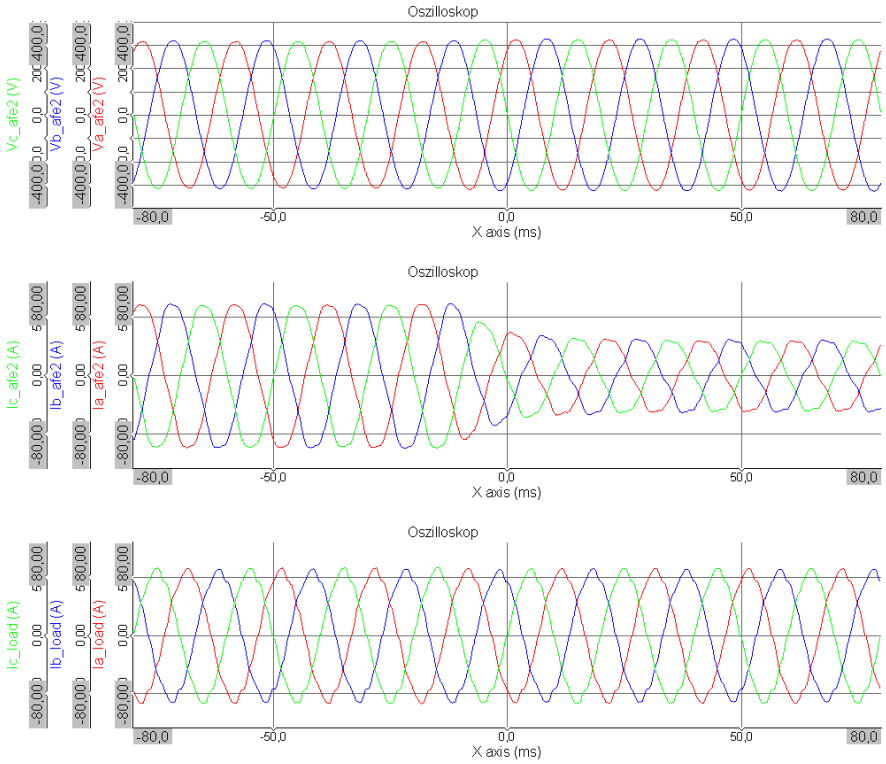

Figure 35: Oscilloscope plot of the AC voltages and currents during the transient load transfer when AFE1 is powered on.

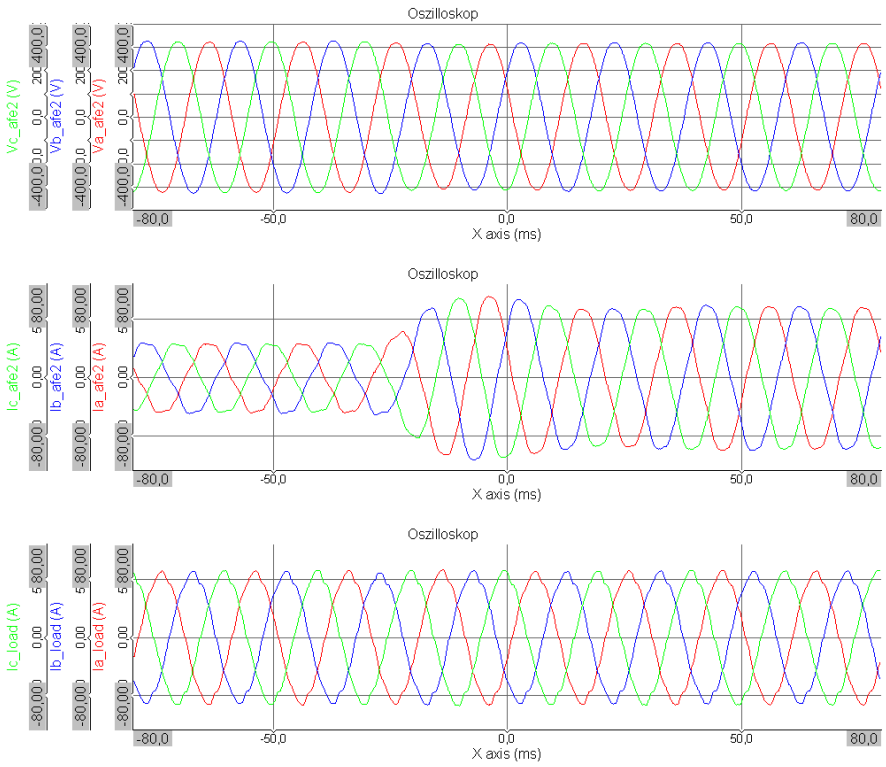

Figure 36: Oscilloscope plot of the AC voltages and currents during the transient load transfer when AFE1 is powered off.

4.5.2 AFE2 powered on and off

As summarised in Table 14, AFE2 starts in the powered off state, while AFE1 supplies all power demanded by the load, P_{LOAD} = 0.8 p.u. The droop factors remain at the settings used for uniform load sharing.

During the test sequence outlined in Table 15, AFE2 is powered on, followed by a transient response of both AFEs, settling at uniform load sharing. Afterwards AFE2 is powered off.

Figure 37 provides an overview over the DC power levels, while Figure 38 shows DC voltages and currents of AFE1 and AFE2.

The transient responses of the AFEs on the DC-side are captured in the oscilloscope plots Figure 39 and Figure 40. The highest voltage-overshoot can be noticed on V_{DCAFE2} during turn-off, amounting to 6 V. I_{DCAFE1} shows the highest current overshoot equalling 3.4 A, also during turn-off.

The power-on process on the AC side of AFE2 can be seen in Figure 41. The power-off sequence of AFE2, captured in Figure 42, leads to an overshoot of its AC voltages as well as ringing on both AC voltages and AC currents. The voltage-overshoot amounts to 65.5 V equalling 20 % of the settled voltage levels.

Table 14: Parameters for the test case exploring the load transfer when AFE2 is powered on and off.

Parameter	Value	Unit
$State_{AFE1}$	ON	n.a.
$P_{MAXAFE1}$	1	p.u.
$Droop_{AFE1}$	1.76	%
$State_{AFE2}$	OFF	n.a.
$P_{MAXAFE2}$	1	p.u.
$Droop_{AFE2}$	1	%
P_{LOAD}	0.8	p.u.
$V_{DC,ref}$	700	V

Table 15: Test Sequence for the test case exploring the load transfer when AFE2 is powered on and off.

Test time	Parameter	Change
t_0	$State_{AFE1}$	ON
t_0	$State_{AFE2}$	OFF
$t_1 \rightarrow t_2$	P_{AFE1}; P_{AFE2}	transient change
t_2	$State_{AFE1}$; $State_{AFE2}$	ON
$t_3 \rightarrow t_4$	P_{AFE1}; P_{AFE2}	transient change
t_4	$State_{AFE1}$	ON
t_4	$State_{AFE2}$	OFF

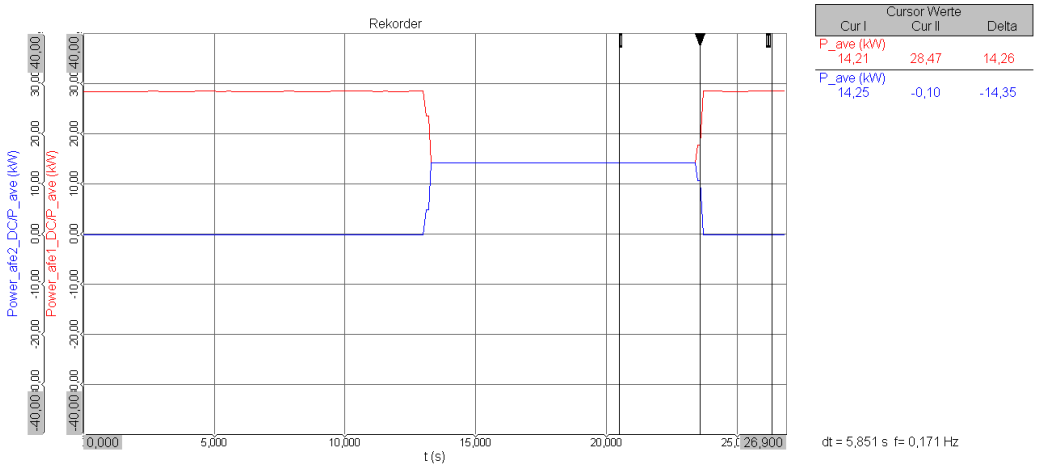

Figure 37: DC power during power off load transfer (AFE2 on/off).

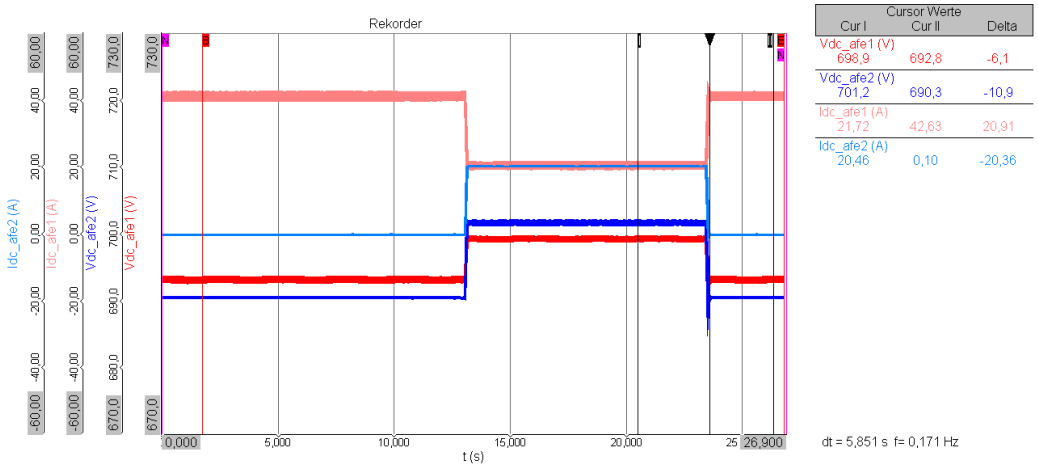

Figure 38: DC voltages and currents during power off load transfer (AFE2 on/off).

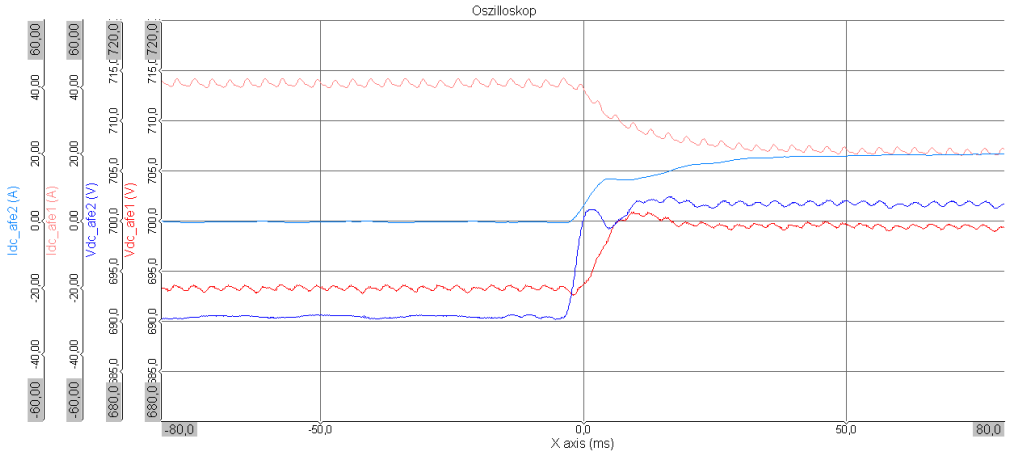

Figure 39: Oscilloscope plot of the DC voltages and currents during the transient load transfer when AFE2 is powered on.

doi:10.5281/zenodo.5115844

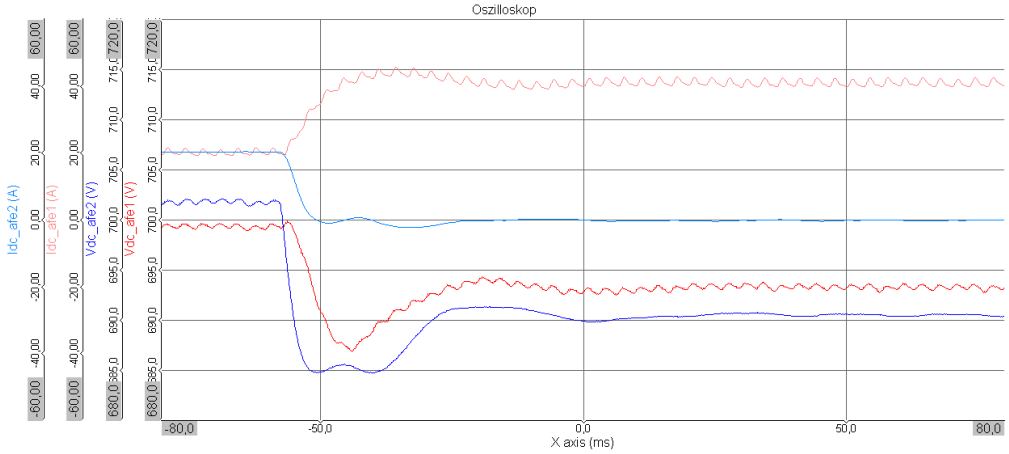

Figure 40: Oscilloscope plot of the DC voltages and currents during the transient load transfer when AFE2 is powered off.

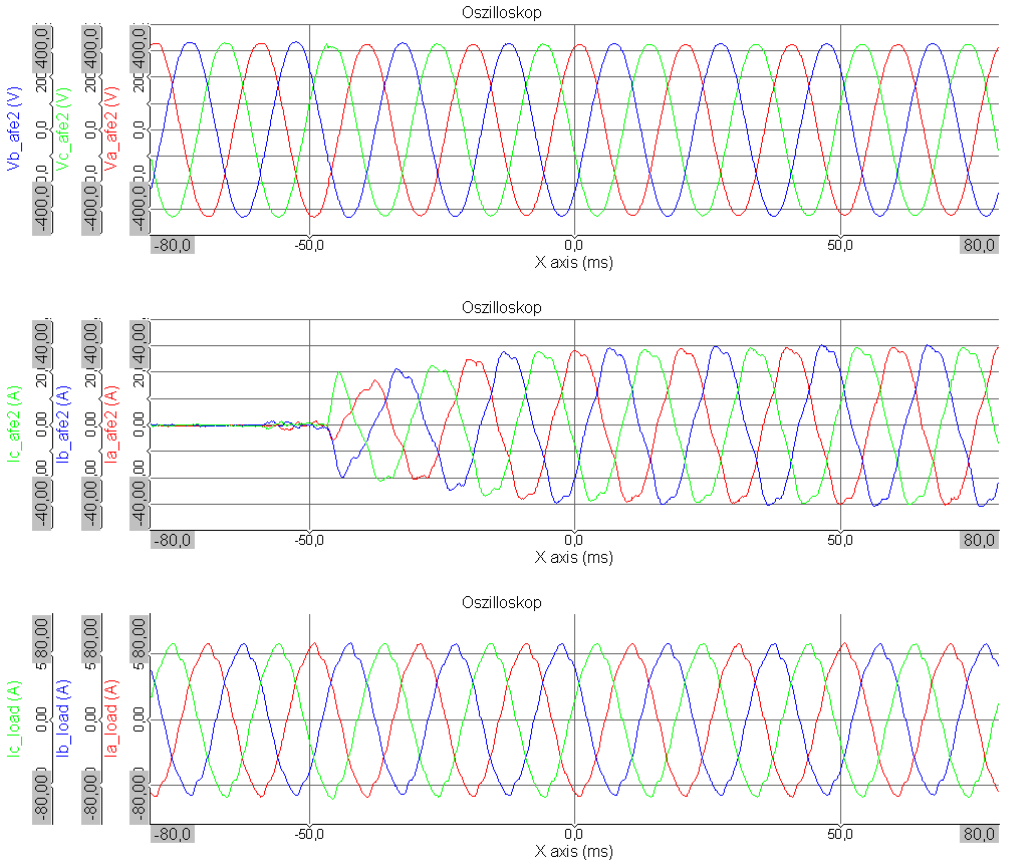

Figure 41: Oscilloscope plot of the AC voltages and currents during the transient load transfer when AFE2 is powered on.

doi:10.5281/zenodo.5115844

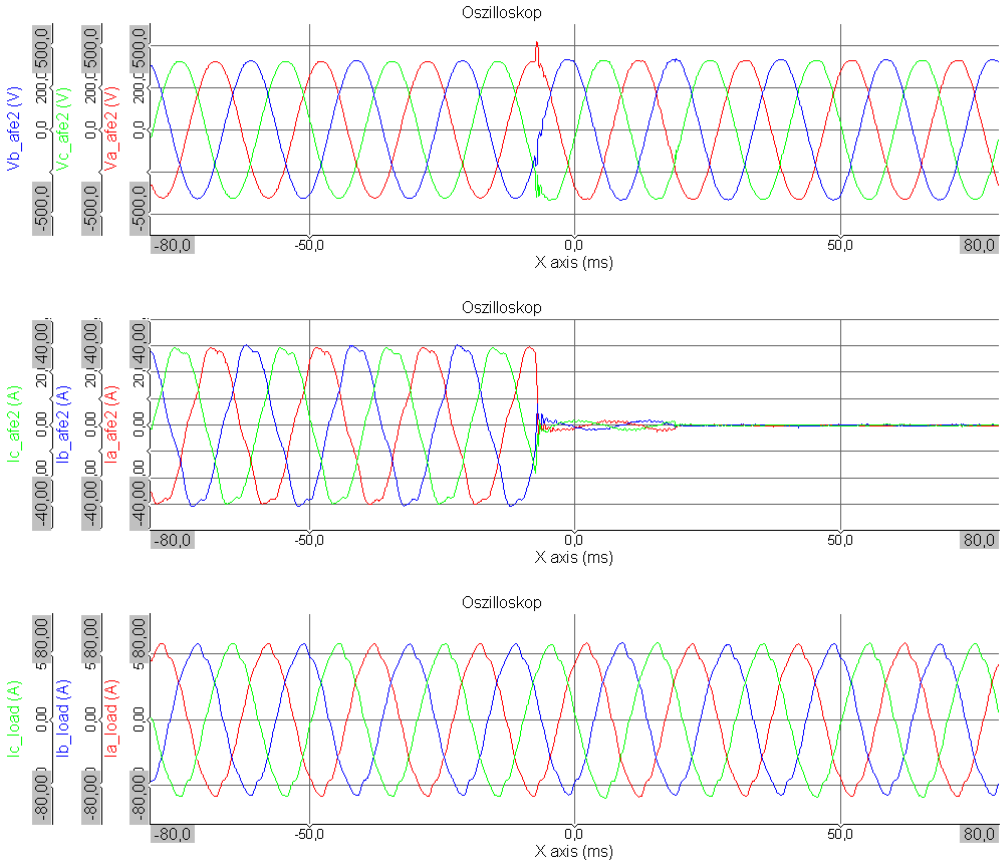

Figure 42: Oscilloscope plot of the AC voltages and currents during the transient load transfer when AFE2 is powered off.

5 Conclusions

As outlined, the control algorithm, the DC droop, developed over the course of this project and implemented on the AIT Smart Grid Converter Active Front End has demonstrated key functionalities required for hybrid AC and DC grids. Those functionalities are bidirectional power flow between AC and DC hybrid grid segments, power sharing between AFEs and capability to provide DC grid power supply redundancy in case one or more AFEs are either disabled or not functional.

Some future considerations are to develop a secondary level control, coordinated emergency shut down, increase short circuit capacity and integrate DC bus pre-charge or DC bus black start capability.

The control algorithm developed and its implementation on the ASGC AFE will be validated in the Italian pilot.

References

Hou, X., Sun, Y., Yuan, W., Han, H., Zhong, C., & Guerrero, J. M. (2016). Conventional P-ω/Q-V Droop Control in Highly Resistive Line of Low-Voltage Converter-Based AC Microgrid. *Energies*, *9*(11). doi:10.3390/en9110943

Liu, Y., Han, Y., Lin, C., Yang, P., & Wang, C. (2019). Design and Implementation of Droop Control Strategy for DC Microgrid Based on Multiple DC/DC Converters. In *2019 IEEE Innovative Smart Grid Technologies - Asia (ISGT Asia)* (pp. 3896–3901). doi:10.1109/ISGT-Asia.2019.8881129

Meng, L., Shafiee, Q., Trecate, G. F., Karimi, H., Fulwani, D., Lu, X., & Guerrero, J. M. (2017). Review on Control of DC Microgrids and Multiple Microgrid Clusters. *IEEE Journal of Emerging and Selected Topics in Power Electronics*, *5*(3), 928–948. doi:10.1109/JESTPE.2017.2690219

HYPERRIDE
THE FUTURE OF POWER DISTRIBUTION

Consortium

Disclaimer

All information provided reflects the status of the HYPERRIDE project at the time of writing and may be subject to change.

Neither the HYPERRIDE Consortium as a whole, nor any single party within the HYPERRIDE Consortium warrant that the information contained in this document is capable of use, nor that the use of such information is free from risk. Neither the HYPERRIDE Consortium as a whole, nor any single party within the HYPERRIDE Consortium accepts any liability for loss or damage suffered by any person using the information.

This document does not represent the opinion of the European Community, and the European Community is not responsible for any use that might be made of its content.

Copyright Notice

This project has received funding from the European Union's Horizon 2020 research and innovation programme under Grant Agreement No. 957788.